

Application of TiO₂-Bayah Natural Zeolite Composite for Degradation of Ammonia Gas Pollutant

TIUR ELYSABETH^{1,✉}, ZULNOVRI¹, GINA RAMAYANTI², SETIADI³ and SLAMET^{3,*}

¹Department of Chemical Engineering, Universitas Serang Raya, Serang, Indonesia

²Department of Industrial Engineering, Universitas Serang Raya, Serang, Indonesia

³Department of Chemical Engineering, Faculty of Engineering, Universitas Indonesia, Depok, Indonesia

*Corresponding author: E-mail: slamet@che.ui.ac.id

Received: 12 November 2018;

Accepted: 6 January 2019;

Published online: 28 June 2019;

AJC-19430

This study aimed to apply the TiO₂-zeolite composite material as a photocatalyst in the photodegradation of ammonia gas. TiO₂-Bayah natural zeolite was synthesized by slurry method and continued with calcination process at 500 °C for 3 h. The amount of TiO₂ varied (5, 10 and 20 % wt) in the total weight of the catalyst to prove the effect of TiO₂ loading on the composition, structure and surface area of the composite, as well as the efficiency of ammonia gas degradation. X-ray fluorescence characterization showed the increasing of TiO₂ composition of composite materials according to the amount of TiO₂ loaded. X-ray diffraction showed that there was no change in the structure of the zeolite before and after combination with TiO₂. BET analysis showed that the composite surface area was larger than the zeolite surface area, but the surface area decreased with increasing TiO₂ loading. Performance test results showed that TZ5 (5 % TiO₂-zeolite) degraded ammonia gas better than other samples.

Keywords: TiO₂-zeolite, Natural zeolite, Ammonia degradation, Gas pollutant.

INTRODUCTION

Ammonia is one of the odorous air pollutants that can interfere with the comfort of the people around it [1]. Ammonia has a adverse effect on humans, animals and the environment because it causes irritation of the nose, throat and respiratory disorders. If the concentration of ammonia in the environment is higher than 300 ppm, it can cause death [2,3]. Indirectly, ammonia affects the formation of ground level ozone and fine ammonium nitrate particulates. Ammonium nitrate particulates and ammonium ions can cause soil damage and eutrophication [4]. The agricultural and livestock sector is a large source of ammonia emissions and is expected to double by 2050 [4-6]. Therefore, it is desirable to explore now and effective method to reduce ammonia emissions.

Ammonia treatment can be done by several methods such as nitrification and denitrification [7], ion exchange [8], membrane technology [9] and adsorption [4,10,11]. But these methods are inefficient and some produce a secondary pollutants [12]. An alternative method that is also being developed is photocatalysis, which is the process of ammonia degradation with

the help of catalysts and photon rays. The catalyst used is a semiconductor that can absorb photon light so as to produce electrons and holes that initiate the formation of hydroxyl groups. This hydroxyl group will oxidize ammonia into compounds that are environmentally friendly. Photocatalytic is a promising method for degradation of ammonia due to simple operating system, high efficiency, low operating cost and minimizing secondary pollutants. This method was first used in 1979 by Mozzanega *et al.* [13], when studying NH₃ decomposition using anatase TiO₂ irradiated by UV rays and its still be object to study, especially to N₂ and N₂O formation. In photocatalytic reactions, the holes and electrons generated from the electron excitation process are the most important components. In addition, the hydroxyl group produced from water decomposition oxidizes ammonia to nitrate and nitrogen gas [14].

The degradation of ammonia has also been reported by several researchers [2,12,15-18]. However, this method also has shortcomings, one of which is the low power of semiconductor adsorption of the material to be degraded. The low adsorption capacity of TiO₂ to pollutants causes low efficiency of photocatalytic activity in its application. Therefore, it is

necessary a method that allows photocatalysts to decompose pollutants with high reaction rates by adsorbing more pollutants. The combination of adsorption-photocatalyst is a promising method. When TiO_2 and adsorbent are combined it produces a synergistic effect which causes an increase in the reaction rate [19].

For TiO_2 semiconductors, several supports have been found such as zeolite [19], aluminosilicate [20], LECA [12], perlite [2], oak [21], cotton woven fabrics [22] and activated carbon [23] which are microporous adsorbents. The better the performance of the buffer in adsorbing pollutants and transferring them to the surface of the catalyst, the process of degradation of pollutants in semiconductor catalysts will be more effective. Zeolite is a natural material which is widely available in Indonesia. Zeolites can be used as adsorbents because their crystalline structure is porous and has a large surface area, composed of silica-alumina frames and high thermal stability. After activation and combination, natural zeolites have good activity. Besides that zeolite is low-cost and its presence is quite abundant compared to other adsorbents.

In this study, Bayah natural zeolite from Indonesia will be integrated with TiO_2 so that a composite material with better performance can be obtained. This research will focus on the synthesis of TiO_2 -zeolite composite material and get the right composition to obtain optimal performance. The structure, compositions and surface area of TiO_2 -zeolite composite was analyzed by X-ray diffraction (XRD), X-ray fluorescence (XRF) and BET method. The performance of composite material was examined by photodegradation of ammonia using photoreactor specifically designed for this study.

EXPERIMENTAL

This research used Bayah natural zeolite from Indonesia. The commercial evonik TiO_2 P25 was used as photocatalyst. Chemicals used for modifications of zeolites were demin water, NH_4NO_3 1 M (Merck), Ethanol and TEOS. Material for photodegradation test was used NH_4OH , H_2SO_4 and pressure air.

Preparation of natural zeolite: Natural zeolite was prepared with several physical and chemical stages. Natural zeolite which was in granular form is crushed and sieved to obtain particle size of 2-5 mm. After sieving, zeolite was washed using demineralized water to remove impurities attached to the zeolite. Then the zeolite was filtered to separate impurities that were carried by water. The filtered zeolite was dried out using an oven at a temperature of 120°C for 3 h. The zeolite was soaked in 200 mL of 1 M ammonium nitrate solution for 24 h with stirring and heating for 3 h at 80°C . Zeolite has been soaked in ammonium nitrate was washed using demineralized water. After washing, the zeolite was dried out to evaporate the water that was still attached to the zeolite. Drying was carried out at 120°C for 3 h. The last stage was the calcination process. This process was carried out to open zeolite pores, evaporate the crystalline water contained in the zeolite structure and increase thermal stability. Calcination was carried out at 500°C for 3 h.

Synthesis of TiO_2 -zeolite composite: The synthesis of TiO_2 -zeolite was carried out using the slurry method. TiO_2 P25 was weighed by variance (5, 10 and 20 %) of the total catalyst. Ethanol was added to TiO_2 until dissolved then sonifi-

cation for 30 min. The mixture of TiO_2 and ethanol was added 2 % wt of the TEOS solution then sonification for 30 min. The next step involve the mixing of demineralized water with zeolite. Then the zeolite suspension was mixed into TiO_2 solution and sonification for 30 min. Evaporated the mixture of TiO_2 /zeolite/TEOS by heating at 110°C until the liquid evaporates and the powder forms. Calcinated TiO_2 /zeolite in the furnace at 500°C for 3 h.

Characterization: Chemical composition composite material was analyzed using X-ray fluorescence (XRF) ICCEL 2800 type spectrometer. M04. The XRF characterization was also carried out to determine the amount of TiO_2 in composite material composition. Calculation of composite material surface area was analyzed using the Brunauer-Emmett-Teller (BET) method. This characterization uses the Autosorb iQ quantachrome brand with nitrogen as a gas analysis. The crystallography of composite material was identified using Shimadzu X-ray diffractometer (XRD) 7000 Maxima-X type with the scan rate at 2°min^{-1} over the scan range 10 - 80° and it was operated at 40 KV and 30 mA with the source of X-ray radiation was $\text{Cu Ni}\alpha$ ($\lambda = 0.15406\text{ nm}$). Chemical structure of composite material was investigated by the Fourier transform infrared, Thermo Scientific FTIR type Diamond Nicolet IS 5 in 4000 - 500 cm^{-1} region.

Composite material (TiO_2 -zeolite) performance test: Performance testing of composite materials was carried out on a specially designed photoreactor (Fig. 1). The gas degradation column consists of four UV @ 8 Watt lamps covered by a quartz glass column and pyrex glass. Ammonia gas pollutants were flowed into columns with compressed air flow which has been regulated at 80, 100 and 120 mL/min. Ammonia which was carried by air will flow along the reactor and undergo a degradation process. The gas mixture at the reactor outlet entered into the bubbler and is absorbed by 0.3 % sulfuric acid solution. Samples were taken after 30 min and then quantitatively analyzed by the Nessler method using a UV-visible spectrophotometer with a wavelength of 430 nm.

RESULTS AND DISCUSSION

Characterization of TiO_2 -zeolite composite material: Some terms used to simplify description in the pictures and tables of research results. The terms are: BNZ (Bayah natural zeolite), BMZ (Bayah modified zeolite), TZ5 (5 % TiO_2 -zeolite), TZ10 (10 % TiO_2 -zeolite) and TZ20 (20 % TiO_2 -zeolite).

In this study synthesis and characterization of composite materials was carried out. Natural zeolite Bayah, which has been activated is then combined with TiO_2 photocatalyst to produce TiO_2 -zeolite composites. The synthesis process uses the slurry method. When synthesizing, the TiO_2 -zeolite catalyst was added TEOS as much as 2 % of the weight of the catalyst which was intended to strengthen the adhesion of TiO_2 on the buffer so as to reduce the level of TiO_2 loss from the catalyst surface. TiO_2 weight percent variation in total catalyst weight is 5, 10 and 20 %.

Characterization of composite materials was done by using X-ray fluorescence (XRF), X-ray diffraction (XRD) and BET. This characterization was carried out to determine the composition, crystal structure and surface area of composite materials.

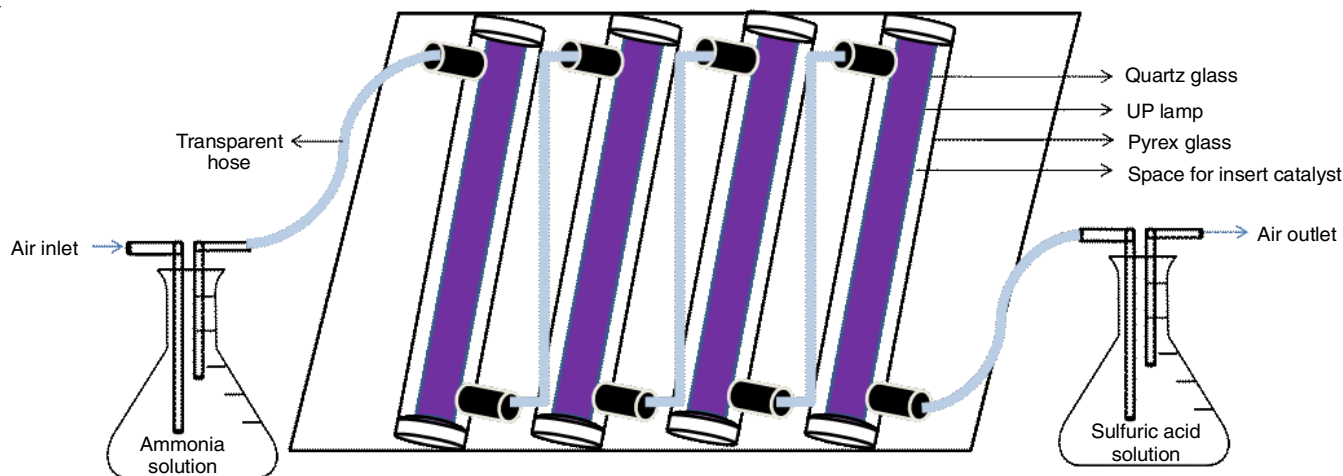


Fig. 1. Photoreactor for degradation of ammonia gas

The XRF characterization results can be seen in Table-1. In the table it was shown that there is an increase in the concentration of TiO₂ in zeolites added by TiO₂. The composition of TiO₂ increased from 0.950 to 18.646 % while the composition of Si and Al decreased after the combination process. It showed that this study has successfully attached TiO₂ to the surface of zeolites. Similar research results were reported by Alshameri *et al.* [24] for the process of phosphate removal using TiO₂/Yemeni natural zeolite.

TABLE-1
CHEMICAL COMPOSITION OF
NATURAL AND MODIFIED ZEOLITES

Compound	Concentration (%)				
	BNZ	BMZ	TZ20	TZ10	TZ5
SiO ₂	64.559	74.700	56.663	64.400	67.402
Al ₂ O ₃	10.621	10.700	6.545	7.636	7.985
TiO ₂	0.950	1.150	18.646	9.75	6.224

To strengthen the adhesion of TiO₂ on the buffer and minimize the occurrence of TiO₂ threshing from the catalyst surface, a TEOS solution was added during preparation. When the catalyst is calcined, the silica contained in the TEOS solution will be activated into an adhesive. In this study TEOS was used as much as 2 % of the total weight of the catalyst. However, the more the amount of TiO₂ from the total weight of the catalyst causes TiO₂ to be more difficult to attach and fall off the surface of the catalyst. This can be seen from the concentration of TiO₂ detected smaller than the initial concentration. Threshing of TiO₂ may be due to the lack of adhesive (TEOS) used. The concentration of TEOS should be adjusted to the amount of TiO₂.

Fig. 2 showed the XRD pattern of various variations of composite material compared to TiO₂ P25 and Bayah natural zeolite. In the figure, it can be seen that TiO₂ P25 showed the characteristic diffraction pattern of anatase phase TiO₂ with minor rutile phase contribution. In the picture, it is also seen the diffractometer from the Bayah natural zeolite and TiO₂/zeolite material. X-ray diffraction results showed that TiO₂ was successfully coated on the surface of zeolites. This can be seen from the main zeolite peak which does not change or is still the same as zeolite before TiO₂ coated [25]. It showed that

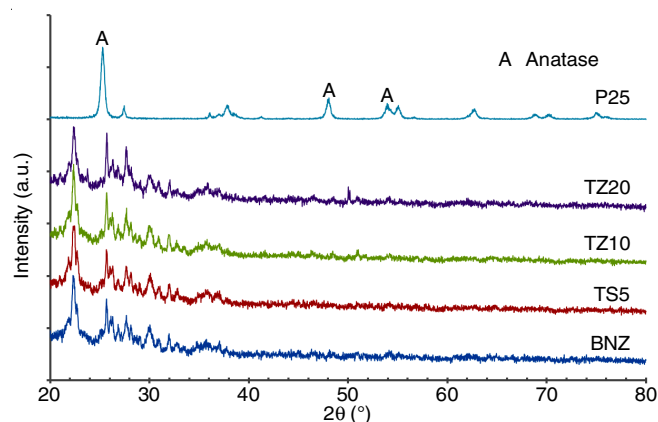


Fig. 2. XRD patterns of the samples

there is no change in the structure of the zeolite when combined with TiO₂. The position of the main peak of natural zeolites is not changed, indicating that the natural structure of zeolites has good thermal stability [24]. Similar XRD patterns for natural zeolites coated with TiO₂ have been reported by Huang *et al.* [26]. Similar diffractograms have also been shown by Jansson *et al.* [19] for composite materials made from TiO₂ with ZSM-5 and zeolite Y. The lack of peak X ray which showed the characteristics of TiO₂ indicates that TiO₂ is dispersed evenly on the surface of zeolite [27]. The XRD pattern of composite material which is identical to natural zeolite also showed that there is no structural damage during the zeolite preparation process. When the TiO₂ content increases to 20 % by weight, the intensity of the diffraction peaks at 48.4° for the anatase phase increases. This phenomenon is in accordance with the results of research obtained by Takeuchi *et al.* [28].

FTIR analysis was carried out to observe the chemical structure of TiO₂-zeolite composites (Fig. 3). The peaks in FTIR spectra did not show any significant changes in the chemical structure of zeolite and composite materials. The hydroxyl groups contained in zeolite could still be observed in TiO₂-zeolite composites. There were OH group and pyrH⁺ at wavenumber 3640 and 1623 cm⁻¹, respectively. The spectra shows that there was a change in the intensity of the hydroxyl group due to the synthesis of TiO₂-zeolite composites. A similar phenomenon was obtained by Eskandarian *et al.* [29].

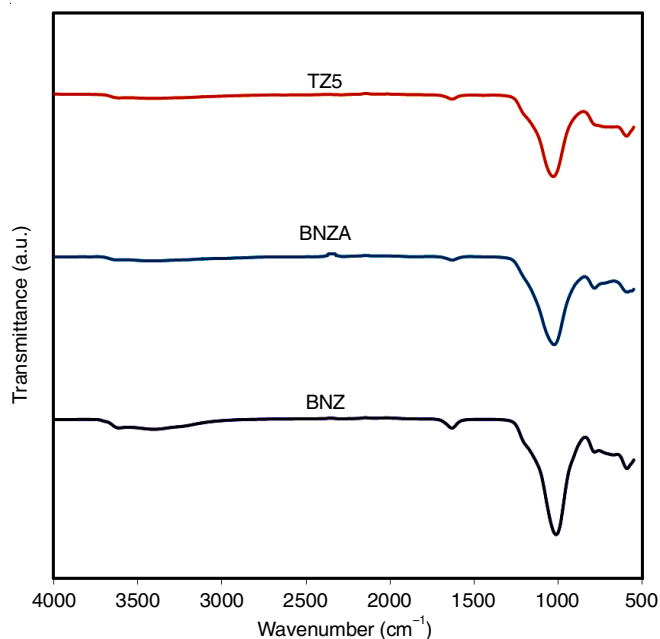


Fig. 3. FTIR spectra of zeolites and composite material

The increasing of surface area can be seen in the N_2 adsorption isotherm curve (Fig. 4). In the figure it can be seen that the volume of N_2 adsorbed by TZ5 is greater than that of other samples. The isotherm adsorption curves of Bayah natural zeolite and TiO_2 -zeolite composites showed the same characteristics. It showed that the zeolite retains its structure despite the addition of TiO_2 . The measurement of surface area was carried out by the BET method and the results can be seen in Table-2. In the table it was shown that the surface area increased after zeolite coated with TiO_2 . The increasing of zeolite surface area after TiO_2 coated was caused by the distribution of TiO_2 throughout the natural zeolite matrix [24]. Nagarjuna *et al.* [30] reported that TiO_2 /Zeolite-4A synthesized by the sol-gel polymerization method has a surface area of $20.8 \text{ m}^2/\text{g}$, this is greater than the surface area of zeolite-4A ($1.2 \text{ m}^2/\text{g}$). According to the results of research conducted by Liu *et al.* [25], surface area and pore volume of TiO_2 /zeolite synthesized by ultrasonication were greater than those without ultrasonication. In this study, the synthesis process is accompanied by ultrasonication at each step. Although it has not been studied further, these results may be used as a reference that the ultrasonication

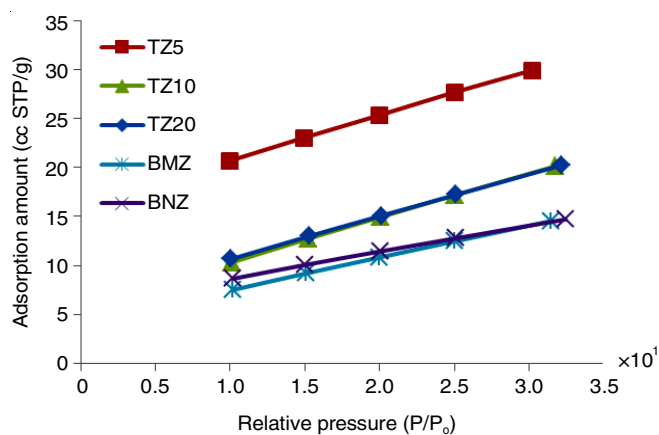


Fig. 4. Nitrogen adsorption isotherms of zeolite and TiO_2 -zeolite at 77 K

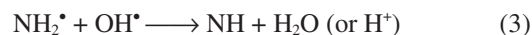
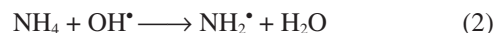
TABLE-2
 TiO_2 -ZEOLITES COMPOSITE SURFACE AREA

Sample	BET surface area (m^2/g)
BNZ	47.450
BNZA	51.525
TZ5	95.213
TZ10	70.840
TZ20	69.093

process can increase the surface area of composite materials. This proves that TiO_2 supported by zeolite can increase surface area and have the opportunity to have higher adsorption capacity.

Photocatalytic performance of composite TiO_2 -zeolite:

When TiO_2 is illuminated by UV light the electrons will be excited from the valence band to the conduction band and form a hole (h^+) in the valence band. Hole is a strong oxidizing agent that can oxidize water molecules to hydroxyl radicals ($\cdot\text{OH}$). Ammonia degradation in TiO_2 -zeolite composites was preceded by the process of adsorption of ammonia into the zeolite pores. In the zeolite pores, NH_3 is bound to H^+ to form NH_4^+ . Then the NH_4^+ molecule will be degraded according to the reaction mechanism given by Altomare *et al.* [14] (eqns. 2-5) as follows:



The performance test of composite material was carried out at a flow rate of 80, 100 and 120 mL/min. Tests carried out for 30 min at room temperature and atmospheric pressure with an initial concentration of ammonia at each flow rate are shown in Table-3. Tests were carried out to see the effect of TiO_2 loading in the catalyst on the photocatalysis process, in this case indicated by a decrease in ammonia concentration that came out of reactor. Ammonia was contacted with a catalyst which had different TiO_2 contents, *i.e.* 0, 5, 10 and 20 % of the total catalyst weight of 10 g per shell of photoreactors with 8 watt UV lights.

TABLE-3
VARIABLE AND PARAMETER OF
AMMONIA DEGRADATION TEST

Flow rate (mL/min)	Time (min)	Volume (Nm^3)	Initial ammonia concentration (mg/Nm^3)
80	30	0.00236	205.97
100	30	0.00295	225.29
120	30	0.00354	230.27

Fig. 5 showed that the addition of TiO_2 in the Bayah natural zeolite causes increased ammonia removal. The presence of TiO_2 on the zeolite surface causes a synergistic effect of the adsorption and photocatalytic processes [19]. This process will take place simultaneously so as to reduce the occurrence of saturation in the zeolite as a result of ammonia accumulation in the pores. This synergistic effect also reduces the desorption

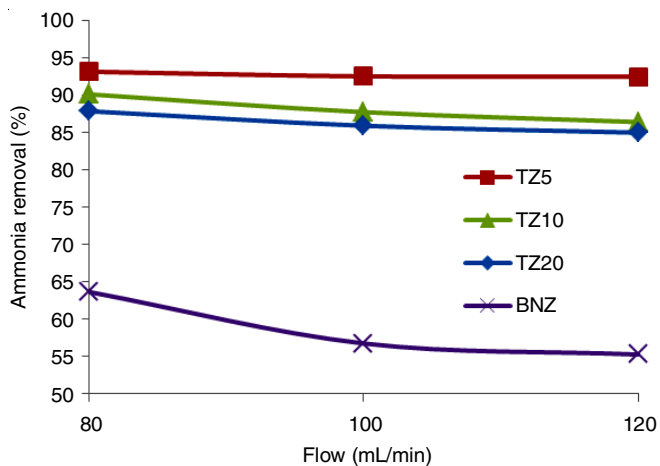


Fig. 5. Effect of loading TiO₂ on ammonia photodegradation at flow rate of 80, 100 and 120 mL/min

of ammonia compounds from the surface of the catalyst because the ammonia which is adsorbed in the zeolite framework will be degraded by TiO₂. Similar results have been reported by Jansson *et al.* [19] that TiO₂ supported by zeolite can increase the degradation of formaldehyde and trichlorethylene.

Fig. 5 shows the effect of the amount of TiO₂ of composition of the composite materials. In the figure, it can be seen that the highest percentage of ammonia removal is done by TZ5. In accordance with the results of BET characterization, TZ5 has the largest surface area so that it can adsorb more ammonia. Ammonia which has been adsorbed into zeolite pores then degraded by TiO₂ which is evenly distributed on the zeolite surface. TZ10 and TZ20 have larger TiO₂ compositions. However, the degradation efficiency of ammonia is smaller than TZ5. The similar results were reported by Rezaei *et al.* [31]. According to the study, too much zeolite loading might cause TiO₂ nanoparticles agglomeration in the zeolite pores to cause pore blockage. In this study the statement can be clarified with the results of the BET characterization which shows that the surface area of the TZ10 and TZ20 is smaller than TZ5. Small surface area can be caused by blockage in the pore. It impacts on the ammonia adsorption process into the zeolite pores. The formation of TiO₂ agglomeration particles can also reduce TiO₂ utilization so that the photocatalytic effect decreases [32].

Fig. 6 showed that the higher the flow rate, the removal percentage of ammonia decreases. This is because the higher the flow rate, so the higher the initial concentration. This is because the higher the ammonia concentration cause the increasing of molecules so that the zeolite pores cannot accommodate more of these molecules. In addition, the increasing number of ammonia molecules means that the more number of holes needed to oxidize ammonia, so that with the use of the same operating conditions, the lower initial concentration of ammonia will make it easier to achieve a smaller output concentration.

Conclusion

In this study the synthesis of Bayah natural zeolite-TiO₂ composite materials was successfully carried out and applied to the ammonia gas photodegradation process. X-ray fluorescence characterization results showed the increasing of TiO₂ composition in the structure of Bayah natural zeolite. However,

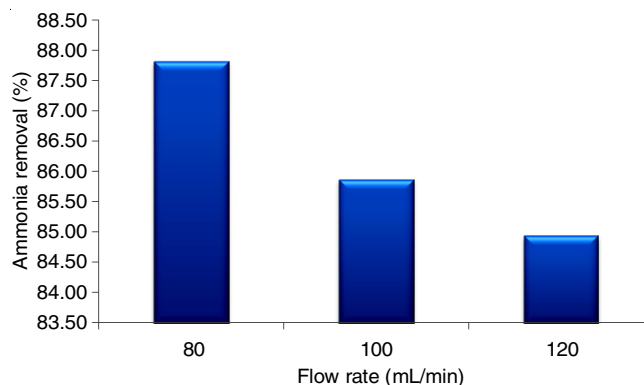


Fig. 6. Effect of flow rate on photodegradation of ammonia for TZ20

the larger composition of TiO₂ on the surface of the zeolite caused the decreasing of surface area. The structure of zeolite did not change even though it was combined with TiO₂ up to 20 % wt. This proved that TiO₂ was uniformly dispersed on the zeolite surface and showed that zeolite had the high thermal stability. In the process of degradation of ammonia, it can be concluded that TZ5 degrades ammonia is more than other composites at a flow rate of 80 mL/min.

ACKNOWLEDGEMENTS

This work was supported by HIBAH PKPT 2018 funded by DRPM Ministry of Research, Technology and Higher Education No. 0795/K4/KM/2018.

CONFLICT OF INTEREST

The authors declare that there is no conflict of interests regarding the publication of this article.

REFERENCES

1. J. Webb, M. Broomfield, S. Jones and B. Donovan, *Sci. Total Environ.*, **470-471**, 865 (2014); <https://doi.org/10.1016/j.scitotenv.2013.09.091>.
2. Y. Shavisi, S. Sharifnia, S.N. Hosseini and M.A. Khadivi, *J. Ind. Eng. Chem.*, **20**, 278 (2014); <https://doi.org/10.1016/j.jiec.2013.03.037>.
3. D. Saha and S. Deng, *J. Chem. Eng. Data*, **55**, 3312 (2010); <https://doi.org/10.1021/je100105z>.
4. E. Rezaei, B. Schlageter, M. Nemati and B. Predicala, *J. Environ. Chem. Eng.*, **5**, 422 (2017); <https://doi.org/10.1016/j.jece.2016.12.026>.
5. S.N. Behera, M. Sharma, V.P. Aneja and R. Balasubramanian, *Environ. Sci. Pollut. Res. Int.*, **20**, 8092 (2013); <https://doi.org/10.1007/s11356-013-2051-9>.
6. F.-X. Philippe, J.-F. Cabaraux and B. Nicks, *Agric. Ecosyst. Environ.*, **141**, 245 (2011); <https://doi.org/10.1016/j.agee.2011.03.012>.
7. M.T. Gutierrez-Wing and R.F. Malone, *Aquacult. Eng.*, **34**, 163 (2006); <https://doi.org/10.1016/j.aquaeng.2005.08.003>.
8. H.-H. Ou, M.R. Hoffmann, C.-H. Liao, J.-H. Hong and S.-L. Lo, *Appl. Catal. B*, **99**, 74 (2010); <https://doi.org/10.1016/j.apcatb.2010.06.002>.
9. M. Darestani, V. Haigh, S.J. Couperthwaite, G.J. Millar and L.D. Nghiem, *J. Environ. Chem. Eng.*, **5**, 1349 (2017); <https://doi.org/10.1016/j.jece.2017.02.016>.
10. W. Zheng, J. Hu, S. Rapoport, Z. Zheng, Z. Wang, Z. Han, J. Langer and J. Economy, *Micropor. Mesopor. Mater.*, **234**, 146 (2016); <https://doi.org/10.1016/j.micromeso.2016.07.011>.
11. A. Qajar, M. Peer, M.R. Andalibi, R. Rajagopalan and H.C. Foley, *Micropor. Mesopor. Mater.*, **218**, 15 (2015); <https://doi.org/10.1016/j.micromeso.2015.06.030>.

12. Z. Mohammadi, S. Sharifnia and Y. Shavisi, *Mater. Chem. Phys.*, **184**, 110 (2016); <https://doi.org/10.1016/j.matchemphys.2016.09.031>.
13. H. Mozzanega, J.M. Herrmann and P. Pichat, *J. Phys. Chem.*, **83**, 2251 (1979); <https://doi.org/10.1021/j100480a014>.
14. M. Altomare, G.L. Chiarello, A. Costa, M. Guarino and E. Selli, *Chem. Eng. J.*, **191**, 394 (2012); <https://doi.org/10.1016/j.cej.2012.03.037>.
15. Y. Shavisi, S. Sharifnia and Z. Mohamadi, *J. Environ. Chem. Eng.*, **4**, 2736 (2016); <https://doi.org/10.1016/j.jece.2016.04.035>.
16. Y. Shaveisi and S. Sharifnia, *J. Energy Chem.*, **27**, 290 (2018); <https://doi.org/10.1016/j.jechem.2017.06.012>.
17. A.C. Sola, D. Garzón-Sousa, J. Araña, O. González-Díaz, J.M. Doña-Rodríguez, P. Ramírez de la Piscina and N. Homs, *Catal. Today*, **266**, 53 (2016); <https://doi.org/10.1016/j.cattod.2015.08.008>.
18. Y. Dong, Z. Bai, R. Liu and T. Zhu, *Catal. Today*, **126**, 320 (2007); <https://doi.org/10.1016/j.cattod.2007.06.034>.
19. I. Jansson, S. Suárez, F.J. Garcia-Garcia and B. Sánchez, *Appl. Catal. B*, **178**, 100 (2015); <https://doi.org/10.1016/j.apcatb.2014.10.022>.
20. M. Nikaido, S. Furuya, T. Kakui and H. Kamiya, *Adv. Powder Technol.*, **20**, 598 (2009); <https://doi.org/10.1016/j.appt.2009.10.003>.
21. N. Tafreshi, S. Sharifnia and S. Moradi Dehaghi, *Process Saf. Environ. Prot.*, **106**, 203 (2017); <https://doi.org/10.1016/j.psep.2017.01.015>.
22. Y. Dong, Z. Bai, R. Liu and T. Zhu, *Atmos. Environ.*, **41**, 3182 (2007); <https://doi.org/10.1016/j.atmosenv.2006.08.056>.
23. S. Yao, J. Li and Z. Shi, *Particuology*, **8**, 272 (2010); <https://doi.org/10.1016/j.partic.2010.03.013>.
24. A. Alshameri, C. Yan and X. Lei, *Micropor. Mesopor. Mater.*, **196**, 145 (2014); <https://doi.org/10.1016/j.micromeso.2014.05.008>.
25. C. Liu, R. Zhang, S. Wei, J. Wang, Y. Liu, M. Li and R. Liu, *Fuel*, **157**, 183 (2015); <https://doi.org/10.1016/j.fuel.2015.05.003>.
26. M. Huang, C. Xu, Z. Wu, Y. Huang, J. Lin and J. Wu, *Dyes Pigments*, **77**, 327 (2008); <https://doi.org/10.1016/j.dyepig.2007.01.026>.
27. S. Suárez, M. Yates, P. Avila and J. Blanco, *Catal. Today*, **105**, 499 (2005); <https://doi.org/10.1016/j.cattod.2005.06.019>.
28. M. Takeuchi, M. Hidaka and M. Anpo, *J. Hazard. Mater.*, **237-238**, 133 (2012); <https://doi.org/10.1016/j.jhazmat.2012.08.011>.
29. M.R. Eskandarian, M. Fazli, M.H. Rasoulifard and H. Choi, *Appl. Catal. B*, **183**, 407 (2016); <https://doi.org/10.1016/j.apcatb.2015.11.004>.
30. R. Nagarjuna, S. Challagulla, N. Alla, R. Ganesan and S. Roy, *Mater. Des.*, **86**, 621 (2015); <https://doi.org/10.1016/j.matdes.2015.07.116>.
31. E. Rezaei, R. Azar, M. Nemati and B. Predicala, *J. Environ. Chem. Eng.*, **5**, 5902 (2017); <https://doi.org/10.1016/j.jece.2017.11.010>.
32. L. Yang, F. Wang, C. Shu, P. Liu, W. Zhang and S. Hu, *Constr. Build. Mater.*, **150**, 774 (2017); <https://doi.org/10.1016/j.conbuildmat.2017.06.004>.